

Center-of-mass energy distributions of coincident H^- and H^+ from the collision-induced dissociation of H_3^+ in He

I. Domínguez, H. Martínez, C. Cisneros, J. de Urquijo, and I. Alvarez

*Laboratorio de Cuernavaca, Instituto de Física, Universidad Nacional Autónoma de México,
Apartado Postal 139-B, 62191, Cuernavaca, Morelos, México*

(Received 25 March 1994)

The collision-induced dissociation of H_3^+ on He at a relative energy of 4.8 keV was performed. The laboratory energy distributions of H^- and H^+ were measured. The energy-analyzed spectrum of H^- was measured in coincidence with H^+ , and the energy-analyzed spectrum of H^+ was measured in coincidence with H^- . From these results, the energy absorbed by the H_3^+ molecule in the excitation process induced by the collision with He previous to its breakup, was evaluated. The center-of-mass energy distributions of both fragments (H^- and H^+) were obtained, and from these the average angle between the positive fragments was determined, as well as the mean total kinetic energy gained by the fragments, and the most probable energy for both charged products. Comparisons with previous measurements are given.

PACS number(s): 34.90.+q, 35.80.+s, 35.20.Gs

INTRODUCTION

An interesting molecular dissociation channel that leads to negative-ion products is the process called polar dissociation. In particular, this process occurs when H_3^+ dissociates as $H^- + 2H^+$, and it has attracted the attention of some experimental and theoretical groups. This interest stems from the need for generating intense negative hydrogen ion beams for neutral beam injection to heat thermonuclear fusion plasmas, and from the theoretical point of view, it is also interesting since the three particle breakup $H^+ + H^- + H^+$ is highly correlated because of the long-range Coulomb interaction forces present in the process.

Earlier experiments on this process were carried out at relative energies in the range of a few keV [1-7,9] with He as a target gas, and assuming that charge transfer from the target is unlikely due to the very small cross section for this process, thus leaving the channel $H_3^+ + He \rightarrow H^+ + H^- + H^+$ as the most feasible one for the production of H^- . Recently [8], one experiment at 2700 keV was performed using Ar as a target, and again it was interpreted by assuming that at this energy the probability of charge transfer is also unlikely and that the main process is that of production of H^- and two protons.

References [1,2] deal mainly with the total cross section for the negative-ion production. References [5,7,8,9] deal with the study of the three body fragmentation. In Refs. [5,9] the internal energy absorbed by the molecule during the dissociation process (Q), and the maximum of the energy distribution (W_{\max}^-) of the H^- fragment were evaluated. Also, the lower value for the correlation angle θ_{12} between the two protons in the center-of-mass (cm) frame of the dissociating H_3^+ molecule was estimated. In Ref. [9], the authors reported coincidence measurements between the negative hydrogen atom and the protons and obtained the energy spectrum of the protons in the H_3^+ cm frame. From these spectra, the most prob-

able energy value of H^+ , W^+ , was found to lie between 0.75 and 4 eV, and the authors could register H^+ counts with energies as high as 9 eV. The results at high energy [8] showed a different behavior; W^+ was found to be 0.89 eV, and the maximum energy of the protons, W_{\max}^+ , was 4.1 eV. Moreover, these authors agreed with some of the results published in Refs. [4,6], concerning the total kinetic energy acquired by the fragments, W_t , and with the maximum energy gain by H^- , W_{\max}^- , during the dissociation process. In principle, there is no reason to believe that in the MeV range of energies with Ar as a target gas the process is exactly the same as that taking place at keV energies with He as a target gas; nevertheless, some affinities between both experiments were found. Because of the similarities and apparent discrepancies between the available sets of data and of the importance of these studies to gain more insight into the understanding of the three-body Coulomb problem, which is far from being complete, it was then decided to undertake these measurements.

In the present paper, we report the results of our recent measurements taken with a apparatus of different geometry from that of Refs. [4,6], allowing the performance of coincidence measurements between the positive and negative fragments, along with a more complete analysis of the H_3^+ fragmentation on He at keV relative energy.

EXPERIMENTAL APPARATUS

A schematic diagram of the experimental apparatus is shown in Fig. 1. A Colutron-type ion source was used to generate the fast-ion beams; these were momentum analyzed by means of a magnetic mass spectrometer and brought to the desired trajectory and energy through a parallel-plate energy analyzer to clean the beam and focus it into the entrance of the interaction cell containing He at a pressure of about 0.1 mTorr. The interaction

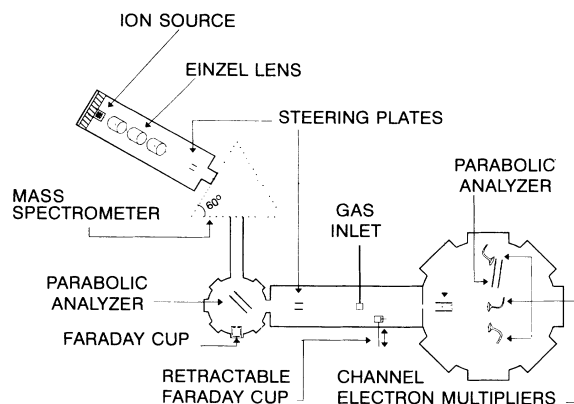


FIG. 1. Schematic of the experimental setup. Not to scale.

cell was a cylinder of 2.5 cm in length and diameter, with entrance and exit collimators of 1.0- and 1.5-mm diameter, respectively; all apertures and collimators had knife edges. The interaction cell was located inside a differentially pumped vacuum chamber. A retractable Faraday cup was located 6 cm away from the exit aperture, allowing for the measurement of the incoming ion-beam current. The dissociation products entered the detection chamber and were charge separated by a perpendicular electric-field produced by a pair of parallel plates, which were located 37 cm away from the gas cell; these plates were rectangular in shape, 5 cm wide and 7.5 cm long and 2.5 cm of separation; a grounded plate with a 0.5-cm-diameter collimator was positioned 2 cm away from the plane defined by the edges of the plates in such a way that the collimator faced the geometrical axis of the volume defined by the plates. The charged fragments, H^- and H^+ , were separated and guided by the field toward their detectors located sideways at $\pm 10^\circ$ from the undeflected beam direction, and 17.4 cm away from the edge of the plates. On one of the sides, a parallel-plate electrostatic analyzer was oriented at 45° between the charged fragment direction and the field, with a channel electron multiplier (CEM) attached to its exit end. A rectangular slit of $0.3 \times 10 \text{ mm}^2$ was placed in front of the CEM, and a collimator of 2.38 mm of diameter at the energy analyzer allowed the measurement of the energy spectrum by sweeping the voltage between its plates. Under these conditions the measured energy resolution, $\Delta E/E$, was 0.01. Two other CEM's constitute the detector system: one of them was placed on the opposite side of the analyzer to register the other charged fragment, and the third CEM at 0° , so that the neutrals could be detected. The detectors and the analyzer were shielded to prevent unwanted events to be registered.

This convenient geometry allowed the measurement of the energy distribution of the charged particles in coincidence, and to monitor the neutral beam in the central detector.

Vacuum base pressures in the system were 10^{-8} Torr without gas in the cell and 8×10^{-7} torr with gas.

The Coincidence Circuit. The coincidence setup that was used for the present investigation has been described

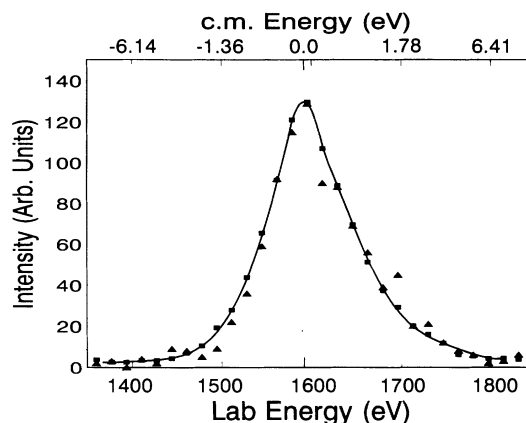


FIG. 2. The squares ■ represent the energy distribution of the H^- fragment taken without the coincidence technique. The triangles ▲ represent the energy distribution of the H^- fragment in coincidence with H^+ . The intensities have been normalized.

in detail in a separate paper [10]. Briefly, it consists of a circuit that triggers a time delay generator upon the arrival of an H^- (or H^+) pulse. During the time it takes for the delay, the gate of the coincidence counter is open. Thus, any ion pulse arriving during this delay time will be acknowledged as a coincidence event, whether it is an H^+ ion from polar dissociation or from any other channel. By reducing the time delay down to 224 ns, which is close to the time it takes for the ion pass through the analyzer, then coincidence spectra such as those shown in Figs. 2 and 3 could be obtained (see below for an explanation). Other counters were attached directly to the amplifiers of the H^- and H^+ channels. The whole setup was computer controlled.

The calibration of the analyzer was performed over the energy range 0.5 to 5 keV, with H^+ , H^- , and H_3^+

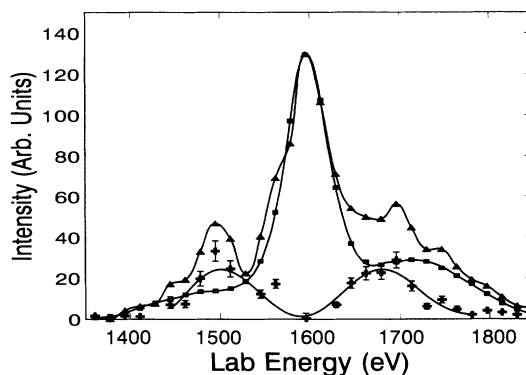


FIG. 3. The squares ■ represent the energy distribution of the H^+ fragment taken without the coincidence technique. The triangles ▲ represent the energy distribution of the H^+ fragment in coincidence with H^- . The intensities have been normalized. The crosses + correspond to the energy distribution of the H^+ fragment in coincidence with H^- after subtraction of the data with, and without the coincidence technique.

beams. The analyzer was first placed on the accelerator axis (0°) and oriented at 45° between the beam direction and the retarding field with no gas in the cell; then it was placed at an angle of 10° from the accelerator axis and the calibration procedure was repeated. The calibration was tested several times in this latter position during the course of the experiment.

Prior to any energy distribution measurement, a voltage was applied to the charge-state separating plates to divert H_3^+ toward the analyzer with no gas in the target cell, and it was adjusted to correspond with the center of its energy distribution. Then, helium was admitted in the target cell, the neutral fragments were detected in the central detector, and protons and negative hydrogen atoms were diverted to opposite directions to be detected in coincidence. The analyzer voltage was driven by a computer over a range of voltages high enough to cover the complete charged fragment spectra. Thus, when the H^+ fragments were energy analyzed, the H^- fragments were registered by an open channel electron multiplier (CEM). The same procedure was followed by diverting H^- into the analyzer and registering the H^+ by the open CEM.

The coincidence measurements, namely, those of H^+ (or H^-) fragments produced in the interaction cell containing He gas as a function of the energy gained or lost in coincidence with the opposite charged particle, H^- (or H^+) were performed by sweeping the analyzer voltage with a computer-controlled power supply, and simultaneously counting the H^+ (or H^-) pulses in coincidence with H^- (or H^+) from the CEM for each analyzer voltage step.

RESULTS AND DATA ANALYSIS

The data were analyzed according to the following kinematic relations (see Ref. [5] for more details):

$$E_{\text{lab}} = \frac{1}{2}m(V \pm v^-)^2, \quad (1)$$

or its equivalent

$$E_{\text{lab}} = \frac{E_0 - Q}{3} + \epsilon^- \pm 2 \left[\frac{E_0 - Q}{3} \epsilon^- \right]^{1/2}. \quad (2)$$

In these equations, E_{lab} is the H^- energy in the laboratory frame of reference, m is the H^- mass, V represents the cm velocity of H_3^+ after the collision, v^- is the velocity of H^- relative to V , E_0 is the acceleration energy, Q is the energy transferred to the molecular ion and ϵ^- is the H^- energy. This formula is applicable for H^+ by simply interchanging ϵ^- for ϵ^+ and v^- for v^+ .

The H^- spectrum

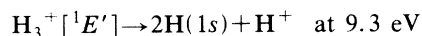
The energy spectrum of H^- was obtained first by passing the negative ion through the calibrated analyzer located at 10° from the accelerator axes and by sweeping the voltage in the plates without operating the coincidence electronics (off mode). The resulting curve is symbolized by the squares in Fig. 2. The coincidence electronics was then set on (on mode) and the H^- counts

were registered according to its energy and in coincidence with H^+ reaching the open detector during the coincidence interval. The counting rate in the second mode was very low (1.5 counts per minute on average). To correlate both spectra, the intensities of their central peaks were normalized. The coincidence counts are represented by the triangles in Fig. 2. After normalization, a replica of the spectra taken with the off mode was obtained. Indeed, it was expected to be this way if the assumption for H^- formation through the available channel $\text{H}^- + 2\text{H}^+$ were true.

A careful inspection of Fig. 2 reveals that the concurrent apexes of both energy distributions are slightly shifted to the left of the position that corresponds to zero energy loss, namely, one third of the incident energy. This shift from the peak at $Q=0$ arises from the loss of energy during the collision, which in turn is a measure of the increment in internal energy of the molecule. From the calibration of the analyzer, and from the spectra, a value of $Q=25 \pm 5$ eV for the energy absorbed by the molecule was determined. This value is close to that reported in Refs. [3,4,6], and it is consistent with the available calculations [9,11].

The H^+ spectrum

In Fig. 3, the continuous line connecting the circles shows the H^+ energy distribution taken in the off mode. Many reaction channels contribute with H^+ fragments to this spectrum; among them, the conspicuous one is the electronic excitation from the $^1A'_1$ to the $^1E'$ energy level. By this process, H_3^+ will dissociate in the following ways [12]



and



This channel was predicted theoretically, including molecular symmetry considerations. The electronic excitation from the $^1A'_1$ to the $^1A'_2$ excited state, and subsequent dissociation can also provide the H^+ fragment at higher energies [13]. These processes contribute with protons mainly to the wings of the spectrum.

On the other hand, the central peak is inconsistent with the electronic excitation process, because it is possible to observe protons with zero-energy release at the positions of the spectrum corresponding to $Q \sim 0$ eV in the cm frame. This is interpreted as a consequence of vibrational excitation of the molecule with subsequent dissociation. The nonvanishing fraction of the primary H_3^+ ions existing at higher vibrational states supplies the initial levels for vibrational excitations connecting the above dissociation limits. Nevertheless, an equilateral triangular H_3^+ may find itself in a different geometry caused by the collision with a target atom. In this new geometry, H_3^+ may be unstable and would decay into H_2 and H^+ . This system in the C_{2v} geometry was studied by Bauschlicher *et al.* [14] over a restricted range of internuclear distances. There are indications of a shallow val-

ley on the potential surface contour diagram corresponding to a stable H_2 and an H^+ at infinity.

The polar dissociation channel, leaving $H^+ + H^- + H^+$ is also present with very small intensity compared with those from the other channels, since the total cross section for H^+ production is $\sim 5 \times 10^{-17} \text{ cm}^2$, as compared with a value of $\sim 7 \times 10^{-19} \text{ cm}^2$ for H^- [2] at 5 keV. When the coincidence setup is in the off mode, all of the above processes contribute to the total intensity of the whole spectrum, that is $I = I' + I'' + \dots + I(2H^+ + H^-)$. In the on mode, preference is given to the latter process among all others since their contribution is not correlated with that of H^- production, which is only possible through the last channel. As a consequence of the very small cross section of the H^- production from polar dissociation ($\sim 7 \times 10^{-19} \text{ cm}^2$ at 5 keV)² the total intensity of the spectrum will be reduced drastically because all those uncorrelated ions that do not happen to reach the detector during the short coincidence interval (224 ns), but the features due to the H^+ ions that were produced simultaneously with the H^- that triggered the coincidence electronic will become apparent. This coincidence spectrum is shown by the triangles in Fig. 3. When both noncoincident and coincident spectra were normalized to the intensity of the central peak, a comparison reveals a remarkable similarity over some portions, namely, in the position of their apexes, the upper width of the central peak and in the outermost part of the wings. On the other hand, the inner part of the wings shows clearly two lateral bulges arising from the contribution of coincident H^+ ions when the coincident circuit was in the on mode. A subtraction of the normalized spectra allows us to cancel the spurious undesirable channels, and thus obtain a clear energy spectrum of the H^+ produced simultaneously with H^- ; this result is also shown in Fig. 3 by the crosses with error bars. The fitting curve through the experimental points was obtained by adjusting the points to a polynomial by least squares. In spite of the poor statistics, the minimum in the center of the fitting curve is displaced from the zero energy loss in the cm frame $Q=0$, which is the same effect already discussed with respect to the H^- energy spectrum in Fig. 2. This displacement gives a value of $Q=23 \text{ eV}$ as the total energy absorbed by the molecule as internal energy, in agreement with the displacement observed from the H^- spectrum. It is clear that the same channels are present in both spectra, but the number of the H^+ correlated with H^- pertaining to the off mode is two orders of magnitude smaller than the whole, and does not affect the final result to any significant extent. The agreement in the position of their apexes at $Q=0$, in the width of their central peaks, and in the shape and intensity of the outermost part of the wings of both spectra after the normalization ensure that these parts are supplied by H^+ from the channels discussed above, other than $I(2H^+ + H^-)$.

The transformation of the energy distributions to the cm frame of H_3^+ (Figs. 2 and 3) of the polar dissociation fragments was performed. Both cm distributions were normalized to encase the same area and are exhibited in Fig. 4. From this figure, the most probable energy of H^-

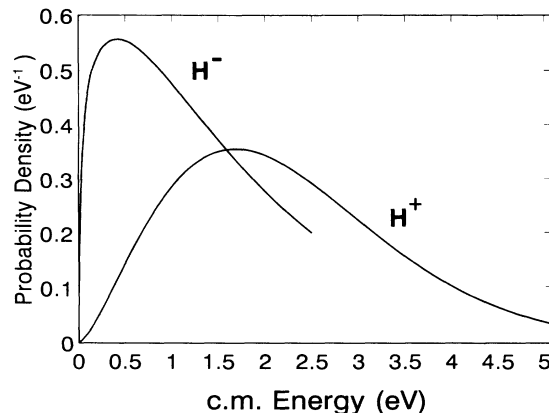


FIG. 4. Transformation of the energy distributions of H^- and H^+ fragments, to the H_3^+ cm frame. Both distributions were normalized to encase the same area.

was found to be 0.42 eV; the maximum, 2.5 eV, was determined by a straight line extrapolation of the trend of the energy distribution shown in Fig. 2. The positive fragment exhibits a maximum at 1.68 eV, which is the most probable energy, and 5.1 eV for the maximum energy value of H^+ .

In fact, that cm distributions represent the probability densities (ρ^+ and ρ^-) for finding a fragment with a given energy ϵ ; both distributions were used to perform the same analysis as in Ref. [8], and by following the same procedure. Thus, in the statistical analysis of these distributions each fragment was allowed any amount of cm energy, provided that the probability for a fragment to possess a certain amount of energy is given by the energy distribution, and that the total cm momentum of the three fragments is zero. The trial function

$$\rho(\epsilon_q) = \alpha \epsilon_q^\beta \exp(-\gamma \epsilon_q^\delta) \quad (3)$$

was used to fit the cm distributions. The parameters α , β , γ , and δ were determined by a least squares procedure to attain the best fit to the experimental points. With these values, the average value of the angle between the two protons was obtained

$$\bar{\theta}_{12} = \int \int \int \rho^+(\epsilon_1^+) \rho^+(\epsilon_2^+) \rho^-(\epsilon^-) \times \arccos \frac{\epsilon^- - \epsilon_1^+ - \epsilon_2^+}{2(\epsilon_1^+ \epsilon_2^+)^{1/2}} d\epsilon_1^+ d\epsilon_2^+ d\epsilon^- \quad (4)$$

and also the average value of the total-kinetic-energy release by the molecule in its fragments

$$\bar{W}_t = \int \int \int \rho^+(\epsilon_1^+) \rho^+(\epsilon_2^+) \rho^-(\epsilon^-) \times (\epsilon_1^+ + \epsilon_2^+ + \epsilon^-) d\epsilon_1^+ d\epsilon_2^+ d\epsilon^- \quad (5)$$

The lower and upper integration limits for the variables ϵ_1^+ and ϵ_2^+ are zero and 5.1, respectively, whereas for ϵ^- , these are zero and 2.5 eV. It was found

$$\bar{\theta}_{12} = 140^\circ \pm 19^\circ$$

and

TABLE I. Summary of the available data of (a) The total-energy loss by the molecule in the collision (Q), (b) The most probable energy value of H^- (W^-), (c) The maximum energy value of H^- (W_{\max}^-), (d) The most probable energy value of the H^+ (W^+), (e) The maximum energy value of H^+ (W_{\max}^+), (f) The total-kinetic-energy release (\bar{W}_t) and the mean angle between the H^+ fragments θ_{12} . The energy values are in eV. * denotes estimated values.

	Ref. [5]	Ref. [9]	Ref. [4]	Ref. [6]	Ref. [8]	Present work
Q	60 ± 12	40	22 ± 6	22 ± 6		25 ± 5
W^-	0.75	0.75	0.5	0.5	0.21	0.42
W_{\max}^-	2.5	3	2.6	3	1.72	2.5
W^+	0.75	4			0.89	1.68
W_{\max}^+	≈ 9	≈ 9			4.1	5.1
\bar{W}_t	$\approx 18^*$	$\approx 18^*$			3.4 ± 1.3	5.5 ± 1.7
θ_{12}	$\approx 163^* \text{°}$	$\approx 163^* \text{°}$			$141^{\circ} \pm 23^{\circ}$	$140^{\circ} \pm 19^{\circ}$

$$\bar{W}_t = 5.5 \pm 1.7 \text{ eV} .$$

The uncertainties reported are the standard deviations of the experimental values.

The present results are shown in Table I together with previously reported data. The comparison must be done by having in mind that the initial state of H_3^+ is unknown, and that the results of Ref. [8] were originated from a high-energy experiment, as opposed to the other experimental results.

CONCLUSION

The H^- and H^+ energy distributions were obtained by applying a coincidence technique. From the first product, H^- , a replica of the spectrum taken with noncoincidence technique was acquired. This test was interpreted as a confirmation that there is only one important channel present in the reaction. Referring to the second product, H^+ , the spectra with the coincidence technique and without it are very different due to the contribution of different channels to H^+ production and the selective effect of the coincidence electronics over the correlated

H^- and H^+ production. From the normalization and comparison of both spectra (on and off modes) it was possible to identify the one that leads to $H^+ + H^- + H^+$, and a clear H^+ energy spectrum was obtained.

A statistical analysis was made employing the transformation to the cm frame of the energy distributions to derive the mean angle between the positive fragments and the mean total-kinetic-energy entailed in the dissociation process. Considering the experimental uncertainties, reasonable agreement is found between the present data and some of the results from different laboratories, as it is observed in Table I, and as it was pointed out before, a comparison between the present results and those from other laboratories must be done by having in mind that the initial states of the projectile are unknown. Nevertheless, the agreement of the present results with those taken at MeV energies with Ar as a target is encouraging.

ACKNOWLEDGMENT

The authors wish to thank Mr. S. Pérez for this technical assistance. This work was partially supported by Grant GDAPA No. IN104391 and CONACYT.

- [1] D. L. Montgomery and D. H. Jaecks, *Phys. Rev. Lett.* **51**, 1862 (1983).
- [2] I. Alvarez, C. Cisneros, J. de Urquijo, and T. J. Morgan, *Phys. Rev. Lett.* **53**, 740 (1984).
- [3] I. Alvarez, H. Martínez, J. de Urquijo, and A. Morales, Two-Electron Phenomena, Second US-México Symposium [Notas Fis. México **10**, 245 (1986)].
- [4] I. Alvarez, H. Martínez, C. Cisneros, A. Morales, and J. de Urquijo, *Nucl. Instrum. Methods Phys. Res. Sect. B* **40/41**, 245 (1989).
- [5] O. Yenen, D. H. Jaecks, and L. M. Wiese, *Phys. Rev. A* **39**, 1767 (1989).
- [6] I. Alvarez, H. Martínez, C. Cisneros, A. Morales, and J. de Urquijo, in *Production and Neutralization of Negative Ions and Beams*, edited by A. Herschcovitch, AIP Conf. Proc. No. 210 (AIP, New York, 1990), p. 135.
- [7] D. H. Jaecks, O. Yenen, D. Calabrese, and L. Wiese, *Atomic and Molecular Physics, Third US-Mexico Symposium* (World Scientific, Singapore, 1991), p. 49.
- [8] N. V. Castro Faria, W. Wolf, L. F. S. Coeino, and H. E. Wolf, *Phys. Rev. A* **45**, 2957 (1992).
- [9] O. Yenen, D. Calabrese, L. M. Wiese, D. H. Jaecks, and G. A. Gallup, *Phys. Rev. A* **47**, 1059 (1993).
- [10] J. de Urquijo, I. Alvarez, I. Domínguez, C. Cisneros, and H. Martínez, *Rev. Sci. Instrum.* (to be published).
- [11] R. S. Gao, L. K. Johnson, G. J. Smith, C. L. Hakes, K. A. Smith, N. F. Lane, R. F. Stebbings, and M. Kimura, *Phys. Rev. A* **44**, 5599 (1991).
- [12] L. J. Schaad and W. V. Hicks, *J. Chem. Phys.* **61**, 1934 (1974).
- [13] K. Kawaoka and R. F. Borkman, *J. Chem. Phys.* **54**, 4234 (1971).
- [14] C. W. Bauschlicher Jr., S. V. O'Neil, R. K. Preston, and H. F. J. Schaefer III, *J. Chem. Phys.* **59**, 1286 (1973).